Journal of Materials Chemistry A

Accepted Manuscript

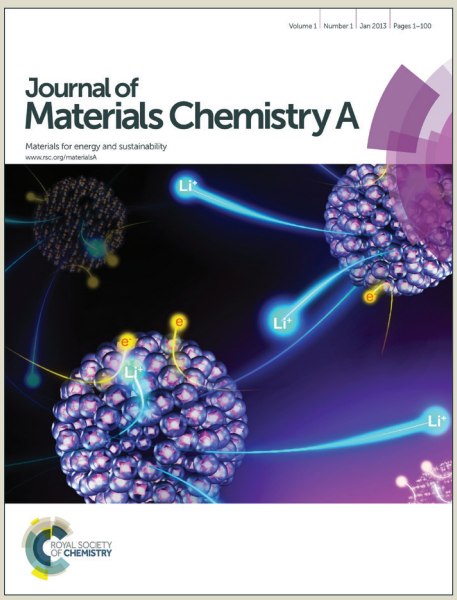

This is an *Accepted Manuscript*, which has been through the Royal Society of Chemistry peer review process and has been accepted for publication.

Accepted Manuscripts are published online shortly after acceptance, before technical editing, formatting and proof reading. Using this free service, authors can make their results available to the community, in citable form, before we publish the edited article. We will replace this *Accepted Manuscript* with the edited and formatted *Advance Article* as soon as it is available.

You can find more information about *Accepted Manuscripts* in the Information for Authors.

Please note that technical editing may introduce minor changes to the text and/or graphics, which may alter content. The journal's standard Terms & Conditions and the Ethical guidelines still apply. In no event shall the Royal Society of Chemistry be held responsible for any errors or omissions in this *Accepted Manuscript* or any consequences arising from the use of any information it contains.

ROYAL SOCIETY OF CHEMISTRY

www.rsc.org/materialsA

Planar Heterojunction Perovskite/$PC_{71}BM$ Solar Cells with enhanced open-circuit voltage *via* (2/1)-step Spin-coating Process

Chien-Hung Chiang[b]; Zong-Liang Tseng [b]; Chun-Guey Wu[a,b,*]

* [a,b] Professor: Chun Guey Wu,
Department of Chemistry, National Central University and
Research Center for New Generation Photovoltaics,
National Central University, Jhong-Li, Taiwan 32001, ROC
Fax: 886-3-4227664
E-mail: t610002@cc.ncu.edu.tw.

[b] Postdoctor: Chien-Hung Chiang; Zong-Liang Tseng
Research Center for New Generation Photovoltaics,
National Central University, Jhong-Li, Taiwan 32001, ROC
Fax: 886-3-4227664.

Journal of Materials Chemistry A Accepted Manuscript

Graphical table of content

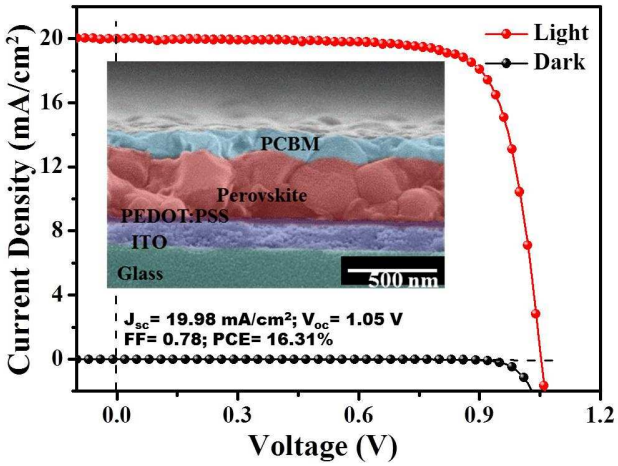

A two-step spin-coating process to synthesize high quality perovskite film at room temperature at ambient atmosphere was reported. Combining optimized PEDOT:PSS hole-transport layer and $PC_{71}BM$ acceptor, the device achieves the power conversion efficiency of 16.31% with a remarkable high Voc of 1.05V and FF of 0.78. The yield of the device is also high, 80% of the devices achieve the efficiency higher than 15%.

Journal of Materials Chemistry A Accepted Manuscript

Perovskite named after Russian mineralogist Lev Perovski is a type of mineral discovered two centuries ago. It was known as a group of materials with interesting magnetic and electric properties. In 2009 Miyasaka *et al.*[1] realized the photovoltaic performance of the organic-perovskites (such as methylammonium lead halide, $CH_3NH_3PbI_3$) when they used very small $CH_3NH_3PbI_3$ nanoparticles to sensitize mesoporous TiO_2 anode. Combining with liquid electrolyte, the resulting device has the PCE of 3 ~ 4%. Four years later (2013), based on the similar cell architecture with solid electrolyte, Grätzel[2] *et al.* and Snaith[3] *et al.* have achieved the remarkable efficiency of above 15%. Beside the phenomenal photovoltaic efficiency, perovskite materials also have the advantages of low cost, high absorption coefficient, excellent carrier transport, tunable compositions and structure as well as can be fabricated by various processing methods.[4,5] Several reports also suggest that solar cells with efficiencies up to 20% are realistically achievable.[6,7] The solution-processable pervoskite photovoltaic devices should be able to compete with the conventional thin-film solar cells on both cost and efficiency. Therefore after the Grätzel's report[2] the research of organic-perovskite based solar cell is burgeoning.

Organic-inorganic pervovskite was first implemented in the mesoscopic dye-sensitized solar (DSC).[1] However, mesoscopic DSC fabrication requires the processing temperature up to 500 ^oC to sinter TiO_2 support, which renders them to be compatible with the flexible substrates. Later studies[8-14] also found that pervovskite can also be applied to the planar heterojunction solar cells which is adaptable for the low temperature solution process. Several film deposition methods were used to fabricate perovskite film in planar heterojunction solar cells, such as co-evaporation of two precursors[3] ($PbCl_2$ and CH_3NH_3I (MAI)), one-step solution process[14] (mixing lead halide and CH_3NH_3I in a solvent before deposition), vapor-assisted solution process,[15] or two-step dipping process.[2]

Journal of Materials Chemistry A Accepted Manuscript

The application of perovskite in organic (small molecule or polymer) solar cell (what professor Snaith named it as an inverted cell architecture) started at 2013. Jeng[16] *et al.* used perovskite as a donor, $PC_{61}BM$ as an acceptor to construct a perovskite/fullerene planar heterojunction hybrid solar cell with the efficiency of 3.9%. The related low photovoltaic performance may be due to the perovskite phase is not pure as revealed by the XRD pattern displayed in the paper. Using similar cell architecture but change the ratio and concentration of PbI_2 and MAI, Lam[17] *et al.* pushed the efficiency of the device to 7.4%. Snaith[18] *et al.* introduced a thin compact TiOx film between $PC_{61}BM$ and Al electrode and used $CH_3NH_3PbI_{3-x}Cl_x$ as an absorber to made the device with efficiency up to 9.8% in 2014. The same year Yang[19] *et al.* used the same absorber $CH_3NH_3PbI_{3-x}Cl_x$ to fabricate a device with 11.5% efficiency and very high fill factor of 0.72. Grätzel[20] *et al.* use a well-designed perovskite cell architecture to achieve an efficiency of 12.04%. They co-evaporated PbI_2 and MAI to prepare perovskite film, insert an electron blocking (polyTPD) layer in-between perovskite and PEDOT:PSS, and used Au as an electrode, the resulting cell has an impressive high open-circuit voltage of 1.05 V. Nevertheless, when the active area of the device enlarged from 0.09 cm^2 to 0.89 cm^2, the efficiency decreased from 12.04% to 8.27% due to the significant decrease in FF value (from 0.67 to 0.52), hence improving the FF in the perovskite based cell is very critical for obtaining high efficiency cell when active area was enlarged.

Planar heterojunction perovskite solar cells have the advantage of simple architecture and hence fabricated easily.[21] All organic-perovskite films used in OPV-typed (inverted) solar cells were fabricated either with one-step solution process[17,18] or co-evaporation method.[20] Very recently, Xiao[22] *et al.* used a interdiffusion method to prepare organic-perovskite films, results in high efficiency and high device yield. In this paper, we present a very similar method (called two-step spin coating process) relating to Xiao (actually our paper is almost ready when we see Xiao's paper) to fabricate highly

Journal of Materials Chemistry A Accepted Manuscript

crystalline $CH_3NH_3PbI_3$ film. Furthermore, we had optimized the quality of PEDOT:PSS layer, therefore high crystalline $CH_3NH_3PbI_3$ film formed at room temperature (in Xiao's paper they heated the PbI_2 and MAI layers to form perovskite by the interdiffusion between two components). In our method, the reaction between PbI_2 and CH_3NH_3I can be well-controlled by the thickness of PbI_2 and the process of adding CH_3NH_3I. Therefore the preparation of perovskite film can be carried out in an ambient atmosphere at room temperature. It has great potential to be used in assembling cost effective, flexible solar cells. The optimized device under AM 1.5 (100 mW/cm^2) radiation achieves the remarkable high conversion efficiency of 16.31% with remarkable high Voc of 1.05V. Device fabrication is also very reproducible: *ca.* 80% of the devices have the efficiency higher than 15% (see Figure S1 of Electronic supporting information (ESI)).

The fabrication steps and architecture of the inverted-type perovskite solar cell reported in this paper is displayed in Figure 1. The detailed preparation procedures and materials used can be found in the experimental section. It is a simplest bilayer planar hetero-junction structure generally used in the organic small molecule solar cells (SMSCs). In this device perovskite, instead of organic small molecule, is used as a light absorber and hole transport layer, PCBM is an electron transport layer. However, there are four Inorganic/Organic interphases in this simple inverted perovskite cell (*vs* two interphases in a typical SMSC). Each interphase should be carefully engineered to obtain high efficiency device. For example we found that high quality PEDOT:PSS dense film can be obtained when ITO substrate was preheated at 120 ^oC for 5 min. On the other hand, PEDOT:PSS film deposited on cold ITO is rough and has some defects (see Figure S2, ESI). Smooth PEDOT:PSS film is essential for fabricating high crystalline/good adhesion $CH_3NH_3PbI_3$ film without defect at room temperature as revealed by SEM micrographs also displayed in Figure S2, ESI. Therefore all devices discussed in this article were fabricated by depositing PEDOT:PSS films in the preheated ITO substrates *via*

Journal of Materials Chemistry A Accepted Manuscript

spin-coating.

In two-step spin-coating process, various thicknesses of PbI_2 films were first deposited on PEDOT:PSS surface from PbI_2/DMF solution by varying the spin rate. Nevertheless when the spin rate is reduced to 1000 rpm, the morphology of the resulting 250 nm PbI_2 film is very rough and also cannot adhere well on the substrate. Therefore, good quality PbI_2 film with thickness of 165 nm (spin rate 1500 rpm) was used for the next fabrication step. To prepare $CH_3NH_3PbI_3$ film, MAI/isopropanol (IPA) solution with concentration range from 10 mg/mL to 50 mg/mL was spin-coated on the top of PbI_2 film at a fixed spin rate of 1500 rpm for 30 seconds and then a layer PCBM was deposited *via* spin coating at ambient atmosphere. One important advantage for fabricating perovskite film with two-step spin-coating method is that the fabrication of PEDOT:PSS/ perovskite/$PC_{61}BM$ can be carried out in an ambient atmosphere at room temperature. After employing Ca/Al electrode using vacuum thermal evaporation, the photovoltaic parameters of the resulting cells were measured and the results were summarized in Table 1. Data in Table 1 reveal that the efficiency of perovskite solar cell is very sensitive to the concentration of MAI/IPA solution. The concentration of MAI affects not only the perovskite formation rate and film homogeneity but also the purity and crystallinity of the resulting $CH_3NH_3PbI_3$ film, which determines the efficiency of the corresponding solar cell. However, in one-step process reported before, PbI_2 and MAI with different stoichiometry were mixed first than spin-coated on the substrate. The formation rate and purity of $CH_3NH_3PbI_3$ depends on the mole ratio of PbI_2 and MAI in one solution. It is difficult to control the formation rate (it will affect the film morphology) and stoichiometry of perovskite separately. On the other hand, the ratio of PbI_2 and MAI and the reaction rate between them can be manipulated individually in two-step process reported in this paper. This is another very important advantage for two-step process. Furthermore two-step (spin-coating of PbI_2 film followed by dipping the film in MAI

Journal of Materials Chemistry A Accepted Manuscript

solution) method has been used to fabricate regular (DSC) typed perovskite solar cell.[2] Dipping process may damage PEDOT:PSS/PbI_2 interface, the resulting cell have low fill factor (unpublished result).

To understand why the concentration of MAI/IPA solution affects the efficiency of the resulting perovskite solar cells, X-ray diffraction patterns of perovskite films on PEDOT:PSS were taken and shown in Figure 2 (the origin 2D data were displayed in Figure S3, ESI). Using lower (36 mg/mL) MAI concentration, the reaction between PbI_2 and MAI is not complete, unreacted PbI_2 was detected. Applying higher (40 mg/mL) MAI concentration, although no PbI_2 exists, a new phase with diffraction peak at 2θ of 10.9 degree appeared. We don't know exactly the structure and components of this new phase, maybe is $CH_3NH_3PbI_3$ intercalated compound. Pure $CH_3NH_3PbI_3$ phase was observed only when the concentration of MAI/IPA solution is *ca*. 38 mg/mL. The peaks appear at 2θ of 13.7, 19.5, 24.0, 27.9 31.4, 40.2, 42.7, and 49.9 degree, indicates the formation of perovskite structure.[23,24] Interestingly, most reported XRD patterns of $CH_3NH_3PbI_3$ film only had three low angle (<35 degree) diffraction peaks at 2θ of 13.9, 28.3 and 31.7 degree, corresponding to the (110), (220) and (310) planes of the tetragonal perovskite structure. Nevertheless, XRD pattern for $CH_3NH_3PbI_3$ prepared with our two-step method has two extra peaks at 19.5 (210) and 24.0 (202) degree. These two diffraction peaks were observed in the simulated perovskite XRD pattern reported by Grätzel[20] *et al.* More diffraction peaks indicated that $CH_3NH_3PbI_3$ film we prepared is highly crystalline. Furthermore, the concentration of MAI also affects the morphology of perovskite film as revealed with SEM micrographs displayed in Figure S4, ESI. Smooth dense perovskite film was observed when the concentration of MAI is close to 38 mg/mL, lower or higher MAI concentration resulting in rough film with some defects.

$PC_{71}BM$ (has good electron mobility[26]) was used to replace $PC_{61}BM$ (mostly common used acceptor in perovskite solar cells) as an electron transporting material and

Journal of Materials Chemistry A Accepted Manuscript

the efficiency of the resulting device increases from 9.92% to 13.29% mainly in the increasing of short-circuit current (*Jsc*, see Table 2). The significantly increase in *Jsc* without changing obviously the open-circuit voltage (*Voc*) and fill factor (*FF*) suggests that the electron transport rate of the acceptor layer has a tremendously effect on *Jsc* and therefore the conversion efficiency (η) of the inverted perovskite solar cell. To further optimize the device, $PC_{71}BM$ layer was solvent annealed (the detailed process was described in the experimental section) at room temperature and the photovoltaic data of the resulting device are also collected in Table 2. Upon solvent annealing of $PC_{71}BM$ layer for 24 h., the efficiency of perovskite cell increases further to 16.31%, the highest efficiency for OPV-typed perovskite solar cell reported today: a significant improvement in both photocurrent (from 18.13 $mAcm^{-2}$ to 19.98 $mAcm^{-2}$), *Voc* (from 0.93 to 1.05 V). Extending the solvent annealing time did not improve the efficiency further.

The *I-V* and IPCE curves for the champion cell (η = 16.31%) are displayed in Figure 3. IPCE curve shows a strong spectral response in the range from 350 nm to 750 nm with efficiency over 80% at the whole wavelength. The integrated current (19.20 $mAcm^{-2}$) from IPCE curve is very close to *Jsc* (19.98 $mAcm^{-2}$) obtained from *I-V* curve. It is notable that the champion cell has good *FF* of 0.78 and remarkable high *Voc* of 1.05 V the highest amongst all perovskite solar cell reported in literature.[27,28] Voc of the champion device is much higher than Xiao's device although FF is slightly lower. We believe that high *Voc* and *FF* (both depend on the series resistance of the device) are the key parameters for achieving such high efficiency for this inverted perovskite solar cells. To explore why the cell prepared with two-step spin-coating method has so high *Voc* and *FF*, the information of the layer stacking in the device (or the morphology of perovskite film in the vertical direction) was investigated. SEM of the cross section of the champion cell (without Ca/Al electrode) was shown in Figure 4. SEM image revealed a well-defined layer-by-layer structure with clear interfaces between each layer. The

Journal of Materials Chemistry A Accepted Manuscript

thicknesses of the PEDOT:PSS, perovskite, and $PC_{71}BM$ layers estimated from SEM pictures are 40 nm, 360 nm (this value is close to that measured with a depth-profile meter), and 140 nm, respectively. The thickness of $CH_3NH_3PbI_3$ and $PC_{71}BM$ layers is similar to those reported by Yang[19] *et al.* but $PC_{71}BM$ layer is much thicker than that for the cell fabricated by Grätzel[20] *et al*. Furthermore, although perovskite film appeared to be composed of the aggregated particles, most particles have the grain size close to the film thickness. Therefore the excitons can diffuse within one single particle (crystallite) to the perovskite/PCBM interphase to perform charge separation and the holes can transport to PEDOT:PSS/ITO anode *via* a single perovskite granule under very low internal resistance. Each layer contacts closely with each other, therefore the interphase resistance is also very low. The series resistance calculated from the I-V curves of the corresponding devices was listed in Table 2. Perovskite solar cell with higher Voc and FF also has lower series resistance. The champion cell reported in this article has a series resistance as low as 4.41 $\Omega.cm^2$. The structure of the cross-section provides a reason to explain why the cell with thick perovskite film and 4 organic/inorganic interphases still have very high *Voc, FF* and therefore high power conversion efficiency.

We found that to achieve the conversion efficiency higher than 15%, high quality (crystalline and pure) perovskite film and solvent annealing of the device are necessary in the inverted perovskite solar cell. To learn more about the effect of the solvent annealing on the photovoltaic performance of the solar cell, Uv/Vis absorption and PL spectra of the device (without Ca/Al electrode) with/without solvent annealing were taken and displayed in Figure 5. Perovskite film has the absorption profile extended to NIR (800 nm) with an absorption coefficient (ε, absorbance divided by the film thickness) of 4.1 x 10^4 cm^{-1} at 550 nm. High ε indicates perovskite film prepared *via* two-step method is very dense.[20, 26] Solvent annealing of $PC_{71}BM$ layer did not change the absorption profile and intensity of preovskite film, on the other hand, the intensity of PL (from the

Journal of Materials Chemistry A Accepted Manuscript

recombination of perovskite excitons) decreased significantly. The decreasing in PL intensity without changing the absorption profile suggested that the increase in *Jsc* may not due to the structure change of perovskite film. Instead, it suggests that electron transfer from perovskite to $PC_{71}BM$ is more efficient, probably due to better perovskite/$PC_{71}BM$ interface contact through solvent annealing. PL intensity of PEDOT:PSS/ perovskite/$PC_{71}BM$ film is almost zero after it was solvent annealed for 1 h indicated that exciton separation and charge transfer was very efficient when perovskite and $PC_{71}BM$ have good contact. However, device with the highest efficiency (16.31%) achieved when perovskite/$PC_{71}BM$ film was solvent annealed for 24 h. (see Table S2). Therefore extending the solvent annealing time may also increase the order of $PC_{71}BM$ film to increase the electron transport rate. Furthermore, perovskite is known as a bipolar absorber (can be as a hole and electron transporter). PL intensities for PEDOT:PSS/ perovskite and perovskite/PCBM films are much weaker than that for glass/provskite film suggests that the charge separation of the exciton can occur in PEDOT:PSS/perovskite and perovskite/PCBM interfaces. Nevertheless, PL intensity for PEDOT:PSS/perovskite is weaker than that for PEDOT:PSS/perovskite, suggesting that perovskite/$PC_{71}BM$ interphase is a better place for excitons to split.

Compared to the photovoltaic parametersof the inverted perovskite cell recently reported by Xaio[22] *et al.* (*Jsc:* 19.6 $mAcm^{-2}$, *Voc:* 0.99 V, *FF:* 0.793 and 15.4% efficiency) or the champion regular perovskite cell reported by Kelly[28] *et al.* (*Jsc:* 20.4 $mAcm^{-2}$, *Voc:* 1.03 V, *FF*: 0.749 and 15.7% efficiency), our device showed the highest open circuit voltage and comparable fill factor and short current, suggesting the importance of the cell interface engineering. $CH_3NH_3PbI_3$ has low exciton binding energy (Eb) (19±3 meV (calculated by Lam[27] *et al.*), much lower than conjugated molecules,[29]) and high conductivity (~ 10^{-3} Scm^{-2}, measured by Grätzel[30] *et al.*). We believe that the thickness of perovskite layer can be further increased or using other derivatives with high

Journal of Materials Chemistry A Accepted Manuscript

electric conductivity (such as $CH_3NH_3PbI_{3-x}Cl_x$) to increase the photocurrent without loss *Voc* and *FF* of the cell is possible. After carefully engineering each layer, inverted (or OSC-typed) planner hetero-junction perovskite solar cell with higher efficiency can be expected in the future.

It was known[31] that some perovskite solar cells showed photocurrent hysteresis at certain voltage scanning rate (or sweep delay time) and scan direction. The photocurrent hysteresis may be due to either the charge traps of the low quality perovskite film, ferroelectric properties of perovskite material and/or the electromigration of ion in perovskites. The efficiency reported for a device with photocurrent hysteresis may not truly represent the performance of the device. We also used different sweep delay time and two opposite scan directions to measure *I-V* curves and the results were displayed in Figure 6. Our perovskite solar cell shows no photocurrent hysteresis at all sweep delay times and scan directions. The results also suggested that the hysteresis in photocurrent is more likely due to the defects or charge traps in perovskite film, which can be solved by the film fabrication process. The device fabricated with our method has a negligible amount of charge traps, therefore has high open-circuit voltage and power conversion efficiency.

In conclusion, we report a two-step spin coating method to synthesize highly crystalline and dense perovskite film with better control in the film stoichiometry and formation rate (it affects the film morphology and charge trap defect of perovskite). Therefore ITO/PEDOT:PSS/perovskite/PCBM can be fabricated in an ambient

Journal of Materials Chemistry A Accepted Manuscript

atmosphere using solution process at low temperature. The champion cell has the power conversion efficiency of 16.31% with remarkable high *Voc* of 1.05V and *FF* of 0.78. The yield of the device is also high: *ca.* 80% of the devices achieve the power conversion efficiency higher than 15%. The results demonstrate that fabricating high efficiency inverted perovskite solar cell in a more controllable way is accomplishable *via* new perovskite film preparation method and carefully interface engineering .

Experimental

Materials and Physicochemical Studies. Aqueous dispersion of PEDOT:PSS (1.3~.1.7 wt%, from H.C. Stark Baytron P AI 4083) was obtained from Heraeus Co. Fullerene derivatives ($PC_{61}BM$ (99.8%) and $PC_{71}BM$ (99.8%)) were purchased from Solenne B. V., Netherlands. PbI_2 (99.999%) was purchased from Aldrich Co. All the above materials were used as received. ITO-covered glass substrates purchased from Merck Co. were photolithographically patterned in our laboratory with $HCl_{(aq)}$. CH_3NH_3I (MAI, 99.99%) was synthesized with the same method published in literature.[30] Uv/Vis absorption and PL spectra were recorded with a Hitachi U-4100 and F-7000 spectrometers, respectively. The thickness of the films was measured with a depth-profile meter (Veeco Dektak 150, USA). Five lines on the 1 cm x 1 cm film were made by carefully scratching with a tip and the average height between the hills and valleys is used to represent the film thickness. GIXRD data were collected in the 2θ range 5 ~ 50 degree on a Brucker powder diffractometer (D8 Discover) using Cu Kα1 radiation equipped with a 2D detector. Scanning Electron Micrograph (SEM) was performed with a Hitachi S-800 microscopy at 15 KV. Samples (surface and cross-section of film on substrates) for SEM imaging were mounted on a metal stub with a piece of conducting tape then coated with a thin layer of gold film to avoid charging.

Journal of Materials Chemistry A Accepted Manuscript

Device Fabrication and photovoltaic performance Measurement. PEDOT:PSS was spin-coated on a heat pretreated patterned ITO under 5000 rpm for 50 sec and then annealed at 120 ^{o}C for 15 min. For depositing perovskite layer, first a layer of PbI_2 was spin-coated on top of PEDOT:PSS coated ITO substrate from 0.5 M DMF solution. After PbI_2 layer dried at air, CH_3NH_3I was spin-coated on top of PbI_2 film from isopropanol solution with various concentrations at spin rates of 1500 rpm to form perovskite structure. Specifically, the highest efficiency device was fabricated with the concentration of CH_3NH_3I/IPA *ca.* 38 mg/mL at the spin rate of 1500 rpm. After perovskite film was formed, 4 wt% PCBM in chlorobenzene was spin-coated onto the perovskite layer at 1000 rpm, 30 sec. Solvent annealing of PCBM layer was performed by covering perovskite/ PCBM film with a petri dish for 24 hours before sending into the vacuum evaporator. All the fabrication procedures were carried in the ambient atmosphere at room temperature Finally, the PEDOT:PSS/perovskite/PCBM film was transferred to a vacuum chamber for coating Ca/Al electrode (20 nm/100 nm). The device area is 0.5 cm x 0.2 cm. *I-V* characteristics of the solar cells were taken using a Keithley 4200 source measuring unit under a simulated AM1.5G light (Wacom solar simulator) at 100 $mWcm^{-2}$ and the light intensity was calibrated by KG-5 Si diode. External quantum efficiency (EQE) or incident photo-to-current conversion efficiency (IPCE) was measured in air. A chopper and lock-in amplifier were used for the phase sensitive detection with QE-R3011 measurement system (Enlitech Inc., Taiwan).

Acknowledgements

Financial support from the National Science Council (NSC), Taiwan, ROC (grand number: NSC101-2113-M-008-008-MY3) was great acknowledged. The devices fabrication was carried out in Advanced Laboratory of Accommodation and Research for Organic Photovoltaics, Ministry of Science and Technology, Taiwan, ROC.

Journal of Materials Chemistry A Accepted Manuscript

Supporting Information Available:

Supplementary data are collected in the Electronic supporting information. This material is available online with the article.

Journal of Materials Chemistry A Accepted Manuscript

References

1. A. Kojima, K. Teshima, Y. Shirai, T. Miyasaka, *J. Am. Chem. Soc.* 2009**, 131**, 6050.

2. J. Burschka, N. Pellet, S.-J. Moon, R. Humphry-Baker, P. Gao, M. K. Nazeeruddin, M. Grätzel, *Nature* 2013**, 499,** 316.

3. M. Liu, M. B. Johnston, H. J. Snaith, *Nature* 2013, **501**, 395.

4. C. Kagan, D. Mitzi, C. A. Dimitrakopoulos, *Science* 1999**, 286**, 945.

5. D. B. Mitzi, *Prog. Inorg. Chem.* 2007**, 48,** 1-121.

6. N-G. Park, *J. Phys. Chem. Lett.* 2013**, 4**, 2423.

7. M. D. McGehee, *Nature* 2013**, 50**, 323.

8. S. D. Stranks, G. E. Eperon, G. Grancini, C. Menelaou, M. J. P. Alcocer, T. Leijtens, L. M. Herz, A. Petrozza, H. J. Snaith, *Science* 2013**, 342**, 341.

9. G. Xing, N. Mathews, S. Sun, S. S. Lim, Y. M. Lam, M. Grätzel, S. Mhaisalkar, T. C. Sum, *Science* 2013**, 342**, 344.

10. J. M. Ball, M. M. Lee, A. Hey, H. J. Snaith, *Energy Environ. Sci.* 2013**, 6**, 1739.

11. W. A. Laban, L. Etgar, *Energy Environ. Sci.* 2013**, 6**, 3249.

12. Y. Zhao, K. Zhu, *J. Phys. Chem. Lett.* 2013**, 4**, 2880.

13. L. Etgar, P. Gao, Z. Xue, Q. Peng, A. K. Chandiran, B. Liu, M. K. Nazeeruddin, M. Grätzel, *J. Am. Chem. Soc.* 2012**, 134**, 17396.

14. G. E. Eperon, V. M. Burlakov, P. Docampo, A. Goriely, H. J. Snaith, *Adv. Funct. Mater.* 2014**, 24**, 151.

15. Q. Chen, H. Zhou, Z. Hong, S. Luo, H.-S. Duan, H.-H. Wang, Y. Liu, G. Li, Y. Yang, *J. Am. Chem. Soc.* 2014**, 136,** 622.

16. J.-Y. Jeng, Y.-F. Chiang, M.-H. Lee, S.-R. Peng, T.-F. Guo, P. Chen, T.-C. Wen*, Adv. Mater.* 2013**, 25***,*** 3727.

17. S. Sun, T. Salim, N. Mathews, M. Duchamp, C. Boothroyd, G. Xing, T. C. Sumbce, Y. M. Lam, T *Energy Environ. Sci.* 2014, **7**, 399.

Journal of Materials Chemistry A Accepted Manuscript

18. P. Docampo, J. M. Ball, M. Darwich, G. E. Eperon, H. J. Snaith, *Nature Commun.* 2014**, 4**, 2761.

19. J. You, Z. Hong, Y. (M.)Yang, Q. Chen, M. Cai, T.-B. Song, C.-C. Chen, S. Lu, Y. Liu, H. Zhou, Y. Yang, *ACS Nano* 2014**, 8**, 1674.

20. O. Malinkiewicz, A. Yella, Y. H. Lee, G. M. Espallargas, M. Grätzel, M. K. Nazeeruddin, H. J. Bolink, *Nat. Photo.* 2014**, 8,** 128.

21. G. E. Eperon, V. M. Burlakov, P. Docampo, A. Goriely, H. J. Snaith, *Adv. Funct. Mater.* 2014**, 24**, 151.

22. Z. Xiao, C. Bi; C. Shao, Q. Dong, Q. Wang, Y. Yuan, Y. Wang, Y. Gao, Y. G. Huang, *Energy Envion.Sci,* DOI: 10.1039/C4EE01138D .

23. A. Kojima, K. Teshima, Y. Shirai, T. Miyasaka, *J. Am. Chem. Soc.* 2009**, 131**, 6050.

24. J.-H. Im, C.-R. Lee, J.-W. Lee, S.-W. Park, N.-G. Park, *Nanoscale* 2011**, 3**, 4088.

25. T. B. Singh, N. Marjanovi´c, G. J. Matt, S. G¨unes, N. S. Saricici, A. M. Ramil, A. Andreev, H. Sitter, R. Schw¨odiauer, S. Bauer, *Org. Electron.* 2005**, 6**, 105.

26. S. Kazim, M. K. Nazeeruddin, M. Grätzel, S. Ahmad, *Angew. Chem. Int. Ed.* 2014, **53**, 2812.

27. P.-W. Liang, C.-Y. Liao, C.-C. Chueh, F. Zuo, S. T. Williams, X.-K. Xin, J. Lin, A. K. Y. Jen, doi:10.1002/ adam.201400231

28. D. Liu, T. L. Kelly, *Nat. Photo.* 2014, **8,** 133.

29. V. I. Arkhipov, H. B¨assler, *Phys. Status Solidi A* 2004, **201**, 1152.

30. L. Etgar, P. Gao, Z. Xue, Q. Peng, A. K. Chandiran, B. Liu, M. K. Nazeeruddin, M. Grätzel, *J. Am. Chem. Soc.* 2012**, 134**, 17396.

31. H. J. Snaith; A. Abate; J. M. Ball; G. E. Eperon; T. Leijtens; N. K. Noel; S. D. Stranks; J. T.-W. Wang; K. Wojciechowski; W. Zhang, *J. Phys. Chem. Lett.* 2014, **5**, 1511.

Journal of Materials Chemistry A Accepted Manuscript

Figure caption:

Figure 1: Preparation step and architecture of the inverted perovskite/PCBM solar cell. (SC.: Spin-coating, TE.: thermal evaporation)

Figure 2: X-ray diffraction patterns for perovskite films prepared with varying MAI concentration and the related compounds (MAI and PbI_2).

Figure 3: *I-V* and *IPCE* curves of the champion perovskite/PCBM solar cell reported in this paper.

Figure 4: SEM diagram of the cross-section for the champion cell without Al electrode.

Figure 5: UV/Vis absorption (a) and PL (b) spectra of PEDOT:PSS/perovskite/ PCBM films before and after solvent annealing. (The PL spectra of glass/perovskite, PEDOT:PSS/perovskite, and perovskite/PCBM films are also shown for references).

Figure 6: (a) I-V curves measured with different delay time between each measuring point. (b) I-V curves measured at different sweep directions.

Journal of Materials Chemistry A Accepted Manuscript

Table 1: Device parameters for the solar cells based on perovskite films prepared with varying MAI concentration.

MAI Conc. (mg/mL)	**Jsc ($mAcm^{-2}$)**	**Voc (V)**	**FF**	**η (%)**
20	8.60	0.27	0.27	0.81
30	8.37	0.51	0.53	2.34
32	9.94	0.80	0.70	5.65
34	11.89	0.85	0.70	7.12
36	13.56	0.90	0.72	8.90
38	14.59	0.91	0.74	9.92
40	13.65	0.90	0.71	8.86
50	9.45	0.78	0.66	5.02

Device architecture: ITO/PEDOT:PSS/perovskite/$PC_{61}BM$/Ca/Al

Thicknesses of PbI_2, PEDOT:PSS, and $PC_{61}BM$ are 165 nm, 40 nm, and 140 nm, respectively.

Journal of Materials Chemistry A Accepted Manuscript

Table 2: Photovoltaic parameters for the solar cells based on varying acceptor and acceptor solvent annealing time.

Acceptor	**Solvent annealing time (hour)**	**Jsc ($mAcm^{-2}$)**	**Voc (V)**	**FF**	**η (%)**	**[a]Rs ($\Omega.cm^2$)**
$PC_{61}BM$	0	14.59	0.91	0.74	9.92	5.60
$PC_{71}BM$	0	18.13	0.95	0.76	13.29	5.41
$PC_{71}BM$	24	19.98	1.05	0.78	16.31	4.41

Device architecture: ITO/PEDOT:PSS/perovskite/PCBM

Thickness of perovskite: 360 nm; thickness of PEDOT:PSS: 40 nm; thickness of PCBM:140 nm.

a. Rs: series resistance which is calculated from the corresponding I-V curves.

Journal of Materials Chemistry A Accepted Manuscript

Figure 1.

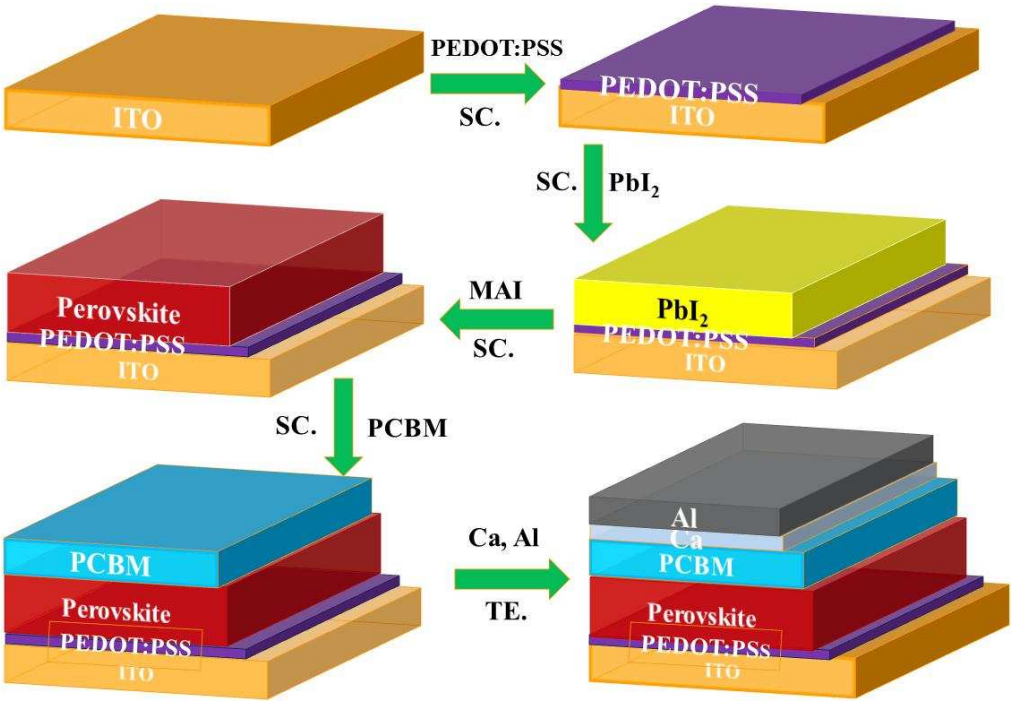

Journal of Materials Chemistry A Accepted Manuscript

Figure 2.

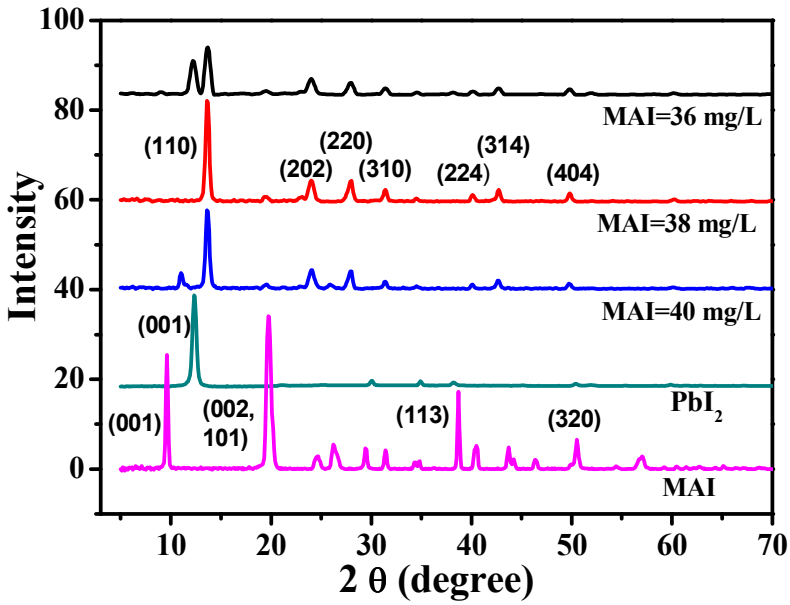

Journal of Materials Chemistry A Accepted Manuscript

Figure 3.

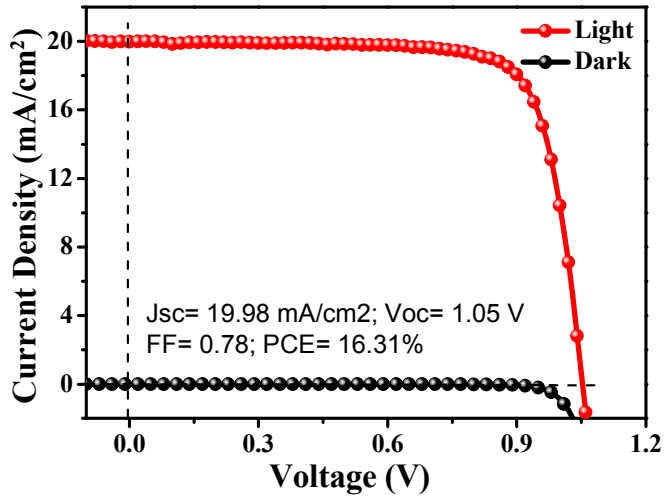

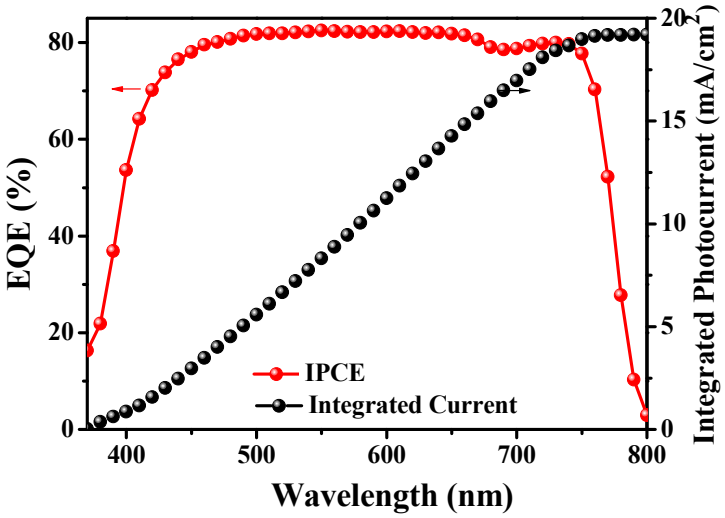

Journal of Materials Chemistry A Accepted Manuscript

Figure 4.

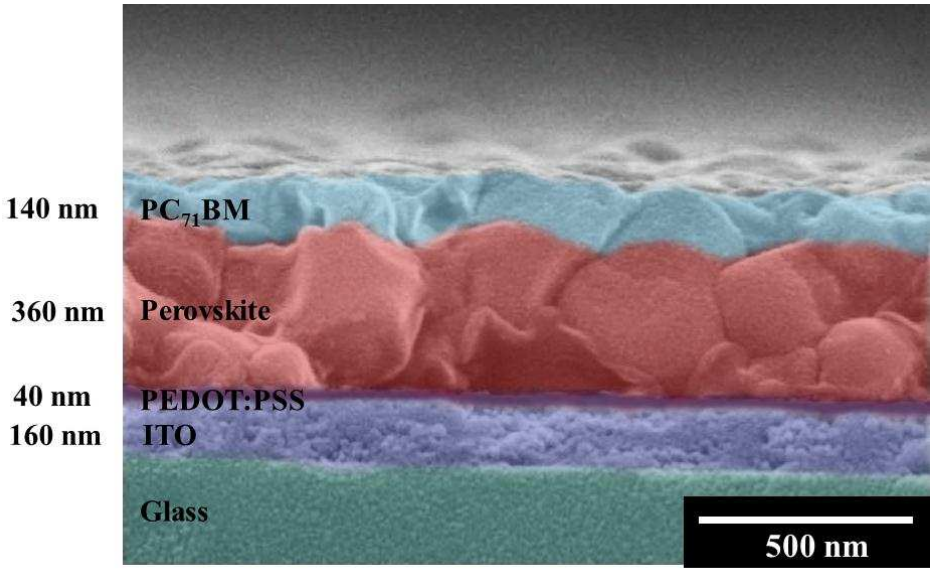

Journal of Materials Chemistry A Accepted Manuscript

Figure 5.

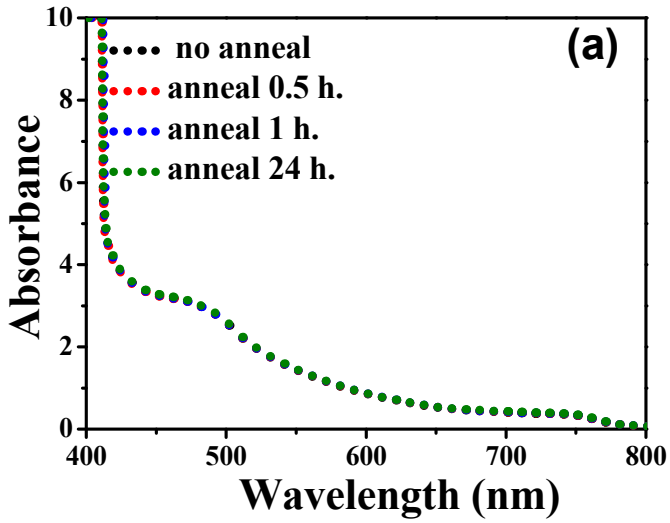

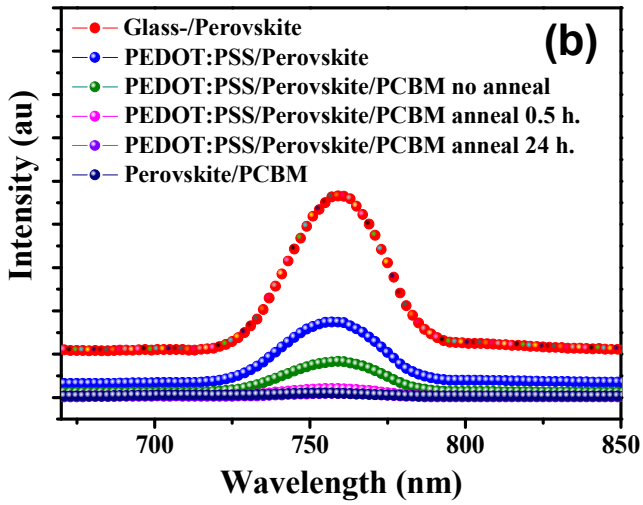

Journal of Materials Chemistry A Accepted Manuscript

Figure 6

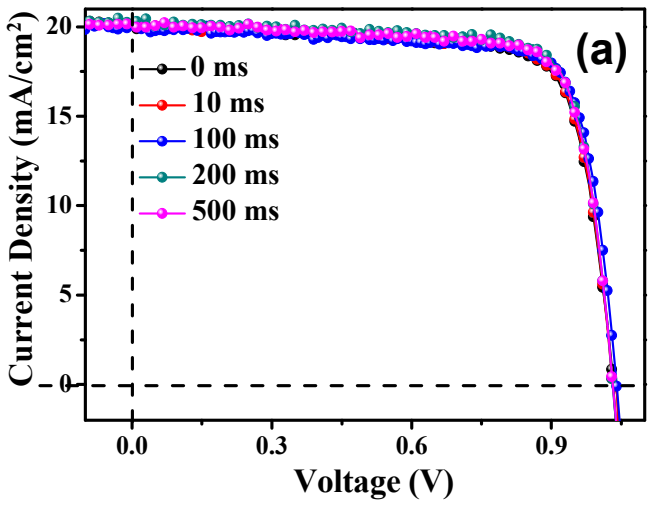

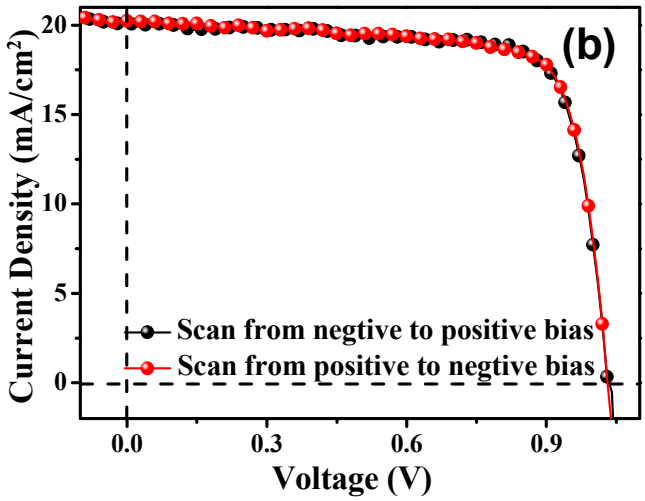

Journal of Materials Chemistry A Accepted Manuscript